

Definition of Spatially Variable Spectral Endmembers by Locally Calibrated Multivariate Regression Analyses

Fabio Maselli*

Linear regression procedures can be applied to derive spectral endmembers using satellite images and superimposed abundance estimates of known components. A common problem, however, is represented by the spatial variability of the spectral endmembers to estimate, which may be caused by variations in several environmental factors (topography, water availability, soil type, etc.). This problem is currently addressed by a modified multivariate regression procedure that can define spatially variable spectral endmembers. The procedure is based on a local calibration of the regression statistics (mean vectors and variance/covariance matrices), which is obtained by weighting the values of the training pixels according to their distance from each pixel examined. The locally found regression statistics are then used to extrapolate pure class spectral endmembers, which are therefore different for each image pixel. An experiment was carried out using multitemporal NOAA-AVHRR NDVI profiles and class abundance estimates of Tuscany region in central Italy. The results show that the spatially variable spectral endmembers are far more accurate than conventional fixed endmembers to recompose the original NDVI imagery. Finally, it is discussed how these spatially variable pure class NDVI values can serve for data integration and as input for agro-meteorological applications and ecosystem simulation modeling. ©Elsevier Science Inc., 2001

INTRODUCTION

The assumption of linearity in the composition of the multispectral signal coming from various scene constituents is

often used to allow a relatively simple treatment of the data acquired (Settle and Drake, 1993; Oleson et al., 1995). The procedures that utilize this assumption rely on the fundamental concept of spectral endmembers, which are the signatures of the constituents that linearly compose the multispectral scene that is being considered (Smith et al., 1990). Ideally, spectral endmembers should represent the signatures of pure elements on the ground, but the term can be applied more broadly to the signatures of cover classes that are sufficiently homogeneous (Lacaze et al., 1996). Spectral endmembers are linked to the properties of the relevant fundamental components and therefore can provide information about these (Richards, 1993). Also, spectral endmembers are commonly used for decomposing the observed scenes by unmixing procedures, thus retrieving the relevant abundance estimates (Smith et al., 1990; Shimabukuru and Smith, 1991; Settle and Drake, 1993). In a similar manner, multitemporal endmembers can be defined by considering time series of a spectral index for spatially stable cover classes. For example, multitemporal profiles of the Normalized Difference Vegetation Index (NDVI) derived from National Oceanic and Atmospheric Administration (NOAA) Advanced Very High Resolution Radiometer (AVHRR) data can be analyzed for different cover classes to assess changes in vegetation phenology and conditions during a certain period (Los, 1998; Genovese et al., 1999).

Several methods have been proposed for the identification of spectral endmembers, but all present evident drawbacks when applied to the analysis of satellite imagery. The use of spectral libraries, for example, requires that the remotely sensed scenes are transformed into actual reflectance values by correcting for atmospheric and topographic effects, which is usually complex and often gives approximate results (Gilabert et al., 1994). Therefore, image-based procedures generally are preferred, which are

* IATA-CNR, P. le delle Cascine 18, 50144 Firenze, Italy

Address correspondence to Fabio Maselli, IATA-CNR, P. le delle Cascine 18, 50144 Firenze, Italy. E-mail: maselli@iata.fi.cnr.it

Received 12 January 2000; revised 1 June 2000.

easily applicable when pure pixels of all main constituents can be found in the scenes. On the contrary, the identification of spectral endmembers is problematic when pure pixels are rare or completely absent in the scene considered (Bateson and Curtiss, 1996; Tompkins et al., 1997; Van Der Meer, 1999). These cases are very common when using low spatial resolution data such as NOAA-AVHRR imagery and are generally addressed by the use of component estimates from external sources analyzed by uni- or multivariate regression techniques (Puyou-Lascassies et al., 1994; Kerdiles and Grondona, 1995; Maselli et al., 1998a). In practice, the component fractions of the classes examined are derived from existing maps or the classification of higher resolution images and are regressed against the spectral values of the low resolution pixels. The spectral signatures of the pure classes are then computed by linearly extrapolating the fraction of each class to 1 (Kerdiles and Grondona, 1995; Maselli et al., 1998a).

Though simple and generally efficient, these methods can not tackle the common cases of spatially variable spectral components. As in fact the conditions of the ground classes can change in space due to several environmental factors (topography, water availability, soil type, etc.), the corresponding spectral signatures can also become spatially variable. Actually, this variability is very common, especially when dealing with broadly defined ground classes. For example, the spectral endmember of a forest class can vary depending on environmental factors such as elevation, slope, aspect, and soil fertility, which affect phenology and growth. In these cases the endmembers found in a relatively large area are no more accurate, which can hamper their utility for scene analysis (Lacaze et al., 1996). Actually, the spatial variability of the spectral endmembers, if not properly accounted for, can introduce errors in the pixel unmixing process and ultimately deteriorate the estimated component fractions (Maselli, 1998; Van der Meer, 1999). Also, as mean spectral endmembers are not representative for the different conditions of a region, their analysis can bring erroneous conclusions on the biophysical properties of the relevant ground elements or classes.

In this work a new methodology is put forward to account for the spatial variability of spectral endmembers. The method is based on a multivariate regression procedure, the statistics of which are defined locally by weighting the training points according to the fuzzy set theory (Zadeh, 1965; Wang, 1990a; Wang, 1990b). This procedure is described here and then applied in a case study to estimate the spatial variability of mean NOAA-AVHRR NDVI profiles of the main cover classes in Tuscany (central Italy). The choice of the case study was due to two main reasons. First, the region is extremely irregular for topography, climate, and land cover, so that the experiment can be considered representative for a situation where the spectral responses of the land surfaces are very variable in space. Second, NOAA-AVHRR NDVI data are linked to several land biophysical properties and have numerous environ-

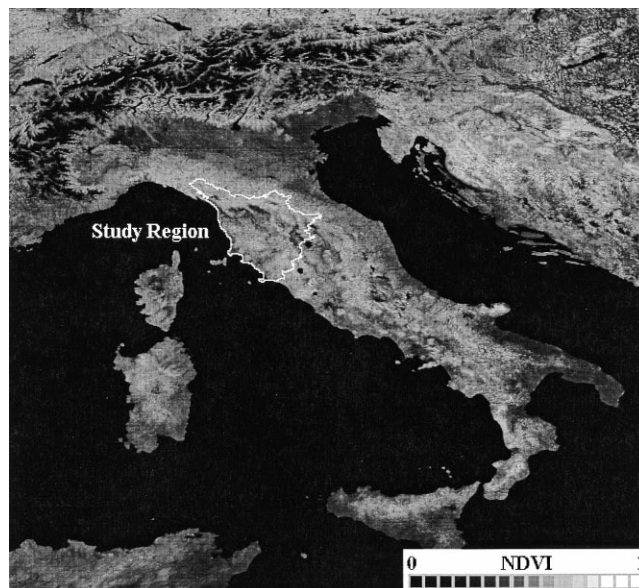


Figure 1. Example of monthly NOAA-AVHRR NDVI MVC image (May 1993) showing the geographical location of Tuscany.

mental monitoring applications (Townshend, 1994; Los, 1998). In particular, NOAA-AVHRR NDVI images are widely applied for vegetation monitoring, even if the relatively low spatial resolution (1.1 km) often complicates their interpretability in heterogeneous areas (Kerdiles and Grondona, 1995; Lacaze et al., 1996). This problem makes the identification of pure class NDVI profiles a particularly challenging task when mixed pixels are prevalent, as is the case in the current investigation. Moreover, NDVI spatial variations can be easily related to environmental controlling factors (topography, climate, etc.), which facilitates the interpretation of the expected results (Maselli et al., 1998b). The results of the experiment were evaluated in comparison to those of a conventional multivariate regression procedure by reconstructing the NDVI images and comparing them to the original data. The utility of the new methodology for operational applications is finally discussed.

STUDY AREA

Tuscany is situated in central Italy between 9° and 12° east longitude and 42° and 44°30' north latitude (Fig. 1). From an environmental point of view, the region is peculiar for its extremely heterogeneous morphological and climatic features. The topography ranges from flat areas near the coastline and along the principal river valleys to hilly and mountainous zones toward the Appennine chain. Approximately two thirds of the region is covered by hilly areas, one fifth by mountains, and only one tenth by plains and valleys.

From a climatic viewpoint, Tuscany is influenced by its complex orographic structure and by the direction of

the prevalent air flows (from west/northwest). As a result, the climate ranges from typically Mediterranean to temperate warm or cool according to the altitudinal and latitudinal gradients and the distance from the sea (Rapetti and Vittorini, 1995). The land use is predominantly agricultural and urban where the land is flat and mixed agricultural and forestry in the hilly and mountainous areas. The main agricultural types are cereal crops in the plains and olive groves and vineyards on the hills. The upper mountain zones are almost completely covered by pastures and forests.

REMOTE SENSING AND ANCILLARY DATA

Reference Data

The land cover classification produced by the European Union (EU) Project CORINE (Annoni and Perdigo, 1997) was utilized as high resolution reference data. The CORINE land cover classification of Tuscany was carried out in 1992–1993 by photointerpretation of several Landsat Thematic Mapper images complemented by panchromatic air photos, all taken during the 1988–1992 period. Information from existing ancillary data (topographic and thematic maps, statistics, etc.) was also considered, so that the CORINE classification was referred to a rather long period and was intended to depict a mean land cover situation. The CORINE nomenclature is hierarchical and comprises three levels common to all countries, with five categories for the first level, 15 for the second, and 44 for the third (Annoni and Perdigo, 1997). The classification provided by the Tuscany Regional Service for Cartography in the form of a vector file with a nominal scale of 1:100,000 was used in the current study.

Satellite Data

AVHRR data transformed in NDVI form were extracted from the archives of Nuova Telespazio (Rome, Italy) within the framework of the EU Project Remote Sensing of Mediterranean Desertification and Environmental Stability (RESMEDES). The archive contains monthly NDVI Maximum Value Composite (MVC) images of 8 years (1986–1993), mapped in a geographic (latitude/longitude) reference system with a 0.01° pixel size (Rossini et al., 1994). The standard procedure for the production of these data comprised the georeferencing of the original images by a cubic convolution algorithm, the radiometric calibration of the first two bands to derive apparent reflectances following Rao and Chen (1994), and the computation of NDVI values to finally obtain the maximum value composites on a monthly basis (Holben, 1986). The final products are therefore 12 monthly NDVI MVCs for each of the eight study years, which were used for the current analysis.

METHODOLOGY

The data processing was mostly carried out using purpose-written programs in Fortran 77 and C languages running

Table 1. Cover classes redefined from the CORINE classification of Tuscany with percentage extensions derived from the relevant map

Class Number	Definition	% Cover
1	Forests	41.5
2	Grassland/shrubland	25.6
3	Tree plantations	5.5
4	Cereal crops	22.4
5	Urban and bare land	5.0

on a Digital Microvax 3500 computer system. Commercial packages such as IDRISI and ENVI were also utilized, running on personal computers equipped with Pentium processors.

Data Preprocessing

The first step of the data processing was to group the CORINE land cover categories into a restricted number of environmentally meaningful classes that could be considered to compute NDVI endmembers (profiles). This was done by taking into account the homogeneity of the expected NDVI profiles (i.e., grouping categories with expected similar profiles). The operation led to the identification of five general classes, which are listed in Table 1. The vector file containing the CORINE land cover classification of Tuscany was therefore reclassified into these five classes and rasterised in a geographic projection with a pixel size of 0.001° . Five Boolean masks were derived from this image, one for each class. These were degraded by pixel aggregation to produce five abundance images with a pixel size of 0.01° superimposed on the AVHRR images.

As previously mentioned, the CORINE classification was referred to a rather long time period, which was almost coincident with the 8 years covered by the available NDVI data (1986–1993). For this reason, the use of mean monthly NDVI data was preferred to the choice of a single year, which would have been arbitrary anyway. Twelve images with mean monthly NDVI values therefore were computed by averaging all original MVC images of the 1986–1993 period.

Conventional Multivariate Regression Analysis

The identification of the NDVI endmembers of the five classes considered was first carried out by conventional linear multivariate regression analysis, which is more efficient than univariate procedures for this objective (Puyou-Lascassies et al., 1994; Maselli et al., 1998a). This analysis implies an assumption of linearity in the composition of the NDVI signal coming from the various scene components, which theoretically should be strictly valid only for the original band values. The linearity assumption, however, was adopted on the basis of recent work, which demonstrated that the use of NDVI data implies only negligible inaccuracies (Kerdiles and Grondona, 1995). Multivariate linear regression models therefore were constructed using

the abundance images of the five classes as independent variables and the mean monthly NDVI images as dependent variables (Anderson, 1984). The development of the multivariate models was carried out by defining unique mean vectors and variance/covariance matrices over the whole study region. The NDVI values corresponding to each pure class then were found by extrapolating the relevant model to 1 cover fraction for the class considered and to 0 for all other four classes (Maselli et al., 1998a).

Locally Calibrated Multivariate Regression Analysis

This approach is a modification of classical multivariate regression procedures applied to the identification of endmembers. As previously mentioned, the rationale for the approach is that the endmember of a land cover class can vary spatially depending on several environmental factors. These variations therefore must be accounted for when identifying endmembers by a multivariate regression procedure. The current idea is that this can be obtained by training and applying the regression models locally (i.e., by considering differently the independent and dependent variables in relation to the distances of the training pixels from each pixel examined).

The mathematical concept for the definition of spatially variable regression statistics is provided by the theory of fuzzy sets. This theory was originally proposed by Zadeh (1965) in opposition to the classical theory of crisp sets and considers that each element of a set can have multiple membership values. According to this, in image analysis fuzzy means and variance/covariance matrices can be computed by giving different weights to each training pixel vector (Wang, 1990a; Wang, 1990b). Since the spatial variability must be currently accounted for, fuzzy statistics can be computed for each image pixel setting the weights as inversely proportional to the pixel distance from the training pixels. In this way, locally calibrated means and variance/covariances can be computed and then used in a multivariate model to identify different endmember values for each image pixel.

Mathematically, a fuzzy multivariate regression model can be constructed by considering different fuzzy statistics for each pixel instead of global means and variance/covariances (Wang, 1990a; Wang, 1990b). In particular, for each pixel examined the fuzzy mean of the independent or dependent variable i , Mean_i^* , is computed as seen in Eq. (1):

$$\text{Mean}_i^* = \frac{\sum W_x V_{x_i}}{\sum W_x} \quad (1)$$

where the summations are over all training pixels, V_{x_i} is the value of the independent/dependent variable i at training pixel X , and W_x is the weight given to the same training pixel, computed on the basis of its distance from the pixel examined (see below).

Similarly, each element of the fuzzy variance/covariance matrices can be found for each pixel examined as (Wang, 1990a; Wang, 1990b) [see Eq. (2)]:

$$\text{Cov}_{ij}^* = \frac{\sum W_x (V_{x_i} - \text{Mean}_i^*)(V_{x_j} - \text{Mean}_j^*)}{\sum W_x} \quad (2)$$

where Cov_{ij}^* is the fuzzy variance/covariance of the independent/dependent variables i and j .

Regarding the weights that define the fuzzy behavior of the model, it is proposed that they can be estimated for each pixel examined with respect to all training pixels by an exponential function of the relevant Euclidean distances as [see Eq. (3)]:

$$W_x = \exp^{-D_x/R} \quad (3)$$

where D_x is the Euclidean distance of the training pixel X from the pixel examined and R is the distance range.

In analogy with spatial analysis (Davis, 1973), the range R is related to the expected spatial variability of the endmembers to identify. In other words, areas where these endmembers are expected to be highly variable should have a low range, while areas where endmembers are probably more homogeneous should have a larger range. A logical consequence of this analogy is that a way to estimate the range can be provided by semivariogram analysis (Davis, 1973). In the current case the range had to model NDVI spatial variations not accounted for by land cover differences, so that the areas that were dominated by a single cover types were first selected as AVHRR pixels with cover fraction of a CORINE redefined class higher than 0.9. Out of these selected pixels, those with most spatially variable NDVI values in the mean annual image were then isolated. Local variance in a 3×3 pixel moving window as defined by Woodcock and Strahler (1987) was used to identify these most spatially variable pixels. In practice, pixels dominated by a single cover type were selected if their local variance was higher than 0.001 NDVI^2 , with this threshold determined empirically. The NDVI values of these pixels were then used for semivariance analysis, which was carried out as described by Pannatier (1994). The fitting of an exponential model to the experimental semivariogram allowed the estimation of a range that, being an expression of the maximum possible spatial NDVI variability, was used for the analysis of all monthly NDVI images.

The locally calibrated multivariate regression procedure was applied to the five abundance images and the 12 mean monthly NDVI images by using Eqs. (1) through (3) to define a fuzzy regression model for each pixel. The extrapolation of the model to 1 cover fraction for each pixel led to the identification of five endmember images corresponding to the expected pure profiles of the five classes considered.

Computation of Reconstructed NDVI Images

The evaluation of the accuracy of the conventional and locally calibrated endmembers was performed by using them and the available class abundance estimates to con-

struct synthetic NDVI images, which were then compared to the original mean NDVI MVC images.

Having the cover class fraction images, a linear composition of the endmember values was computed for each pixel as [see Eq. (4)]:

$$S_NDVI = \sum_{l=1}^{N_c} F_l EM_l \quad (4)$$

where S_NDVI =simulated NDVI value of the pixel, N_c =number of cover classes, F_l =fraction of cover class l derived from the abundance images, and EM_l =NDVI value of endmember l .

This operation was repeated for all 12 mean NDVI MVC images using both the conventional and locally calibrated endmembers. In the latter case, different NDVI values were obviously considered for each pixel, derived from the endmember images previously produced. The resulting synthetic images were then compared to the original NDVI MVCs, and their correspondence was expressed by means of correlation coefficient (r) and root mean square error (RMSE) statistics.

RESULTS

Evaluation of Input Data

The quantitative examination of the CORINE map (Table 1) confirmed that forests, grassland/shrubland, and cereal crops are by far dominant in Tuscany, covering about 41%, 26%, and 22% of the land surface, respectively. The other two classes (tree plantations and urban/bare land) each cover about 5% of the surface and are concentrated in restricted areas. The five abundance images obtained by degrading the CORINE reclassified map are shown in Fig. 2. As can be seen, forests are prevalent in the inner mountain zones, grassland/shrubland and tree plantations are mainly present on the hills, and cereal crops and urban areas are concentrated in the plains.

A visual examination of the 12 NDVI images produced by averaging the original monthly values indicated their good quality. As was expected, the averaging operation reduced possible residual defects of the single images due to radiometric and geometric distortions, so that the final products were more reliable than the original data for subsequent analysis.

Endmembers Identified by Conventional Multivariate Regression Analysis

The NDVI endmembers identified by the conventional multivariate regression procedures are shown in Fig. 3. As can be seen, only the first cover class (forests) has a distinct NDVI profile, while the other three vegetation classes (grassland/shrubland, tree plantations, and cereal crops) have similar profiles. The NDVI profile of urban land is distinct in the first 6 months, but overlaps with the previous three during summer and fall. These profiles can be inter-

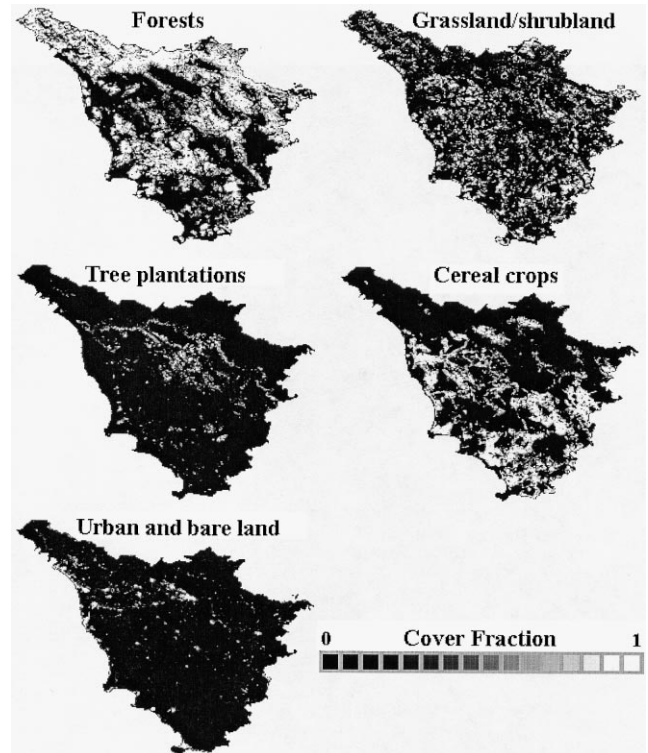


Figure 2. Abundance images derived from the CORINE land cover map of Tuscany reclassified into the five classes listed in Table 1.

preted keeping in mind the eco-climatic conditions of the main regional environments (Maselli et al., 1998b). The temperate-cool climate of the mountain zones favors the photosynthetic activity of forests in summer, when temperature is high and rainfall is not limiting. The Mediterranean climatic features are instead more accentuated on the hills, the valleys, and the plains, where summer aridity increasingly limits vegetation photosynthesis of grassland/shrubland, tree plantations and cereal crops. The NDVI profile of urban areas is obviously the lowest for most of the year, with a small peak in summer due to the presence of irrigated vegetation.

A more in-depth analysis revealed that these NDVI profiles were not completely representative for all pixels in the same cover classes. For example, the NDVI profiles of pure forest pixels located in northern mountain zones were very different from those of pure forest pixels located in southern hills. As previously mentioned, this intraclass NDVI variability can be attributed to two main causes. First, different vegetation types were present within each class (for example, different forest and crop species), each showing slightly different NDVI profiles. Second, there was a certain NDVI variability within each vegetation type caused by several environmental factors (mainly climatic and edaphic), which are known to affect vegetation phenological development and conditions and, consequently, NDVI profiles (Gaston et al., 1994; Maselli et al., 1998b).

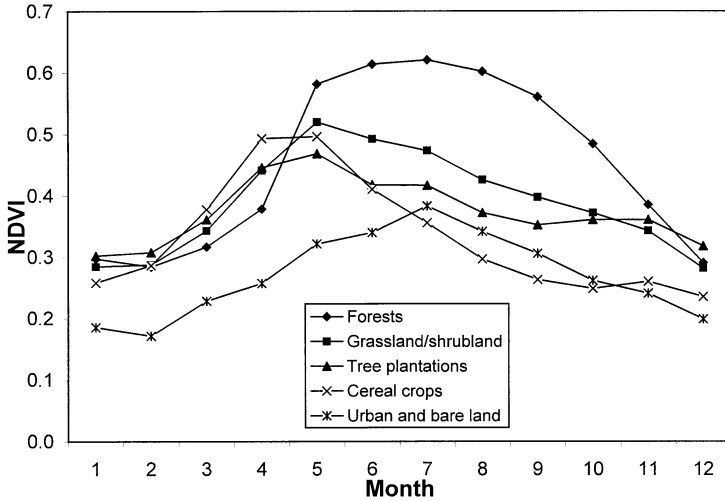


Figure 3. NDVI endmembers of the five cover classes found by the conventional regression procedure.

Endmembers Identified by Locally Calibrated Multivariate Regression Analyses

The experimental semivariogram found using the most spatially variable NDVI values of homogeneous areas is shown in Fig. 4, together with the fitted exponential model. As can be seen, a range of about three pixels was identified, which was deemed reasonable to allow a certain spatial variability in the definition of the fuzzy multivariate regression model by Eq. (3) without introducing too much noise due to NDVI anomalies. In fact, it must be kept in mind that a very small range (less than two to three AVHRR pixels) should have resulted in an extremely localized estimation of regression parameters, with a consequent increase of the importance given to possible anomalous single pixel NDVI values. Also, a smaller range would have led to a very low consideration of the training pixels far from each pixel examined, with a consequent instability of the estimation process in areas where some classes are rare.

According to what was explained in the methodology section, every endmember image produced by the locally calibrated regression analysis can be interpreted as the NDVI values that the corresponding class would have if it covered completely the region, which is obviously an abstraction for pixels located in areas where the class is

very rare or absent. Some examples of these endmember images for two representative cover classes (forests and cereal crops) in winter, spring, and summer months are displayed in Fig. 5. A marked intraimage NDVI variability can be clearly appreciated, which is mostly attributable to the previously mentioned geographical variability in vegetation types and environmental factors influencing the NDVI profile of each cover class. In effect, it can be noted that the main NDVI variations within each class are associated with variations in topography, latitude, and distance from the sea, which are known to be major factors affecting vegetation conditions and development in the region (Maselli et al., 1998b). Wide differences also exist in the endmember images of the classes for the same months, especially in August. This indicates the efficiency of the methodology in separating the NDVI values of the various classes.

Evaluation of Reconstructed NDVI Images

Examples of the original and synthetic NDVI images obtained by recombining the conventional and locally calibrated spectral endmembers are shown in Fig. 6 for the three representative months (February, May, and August), together with the original NDVI images. A first visual

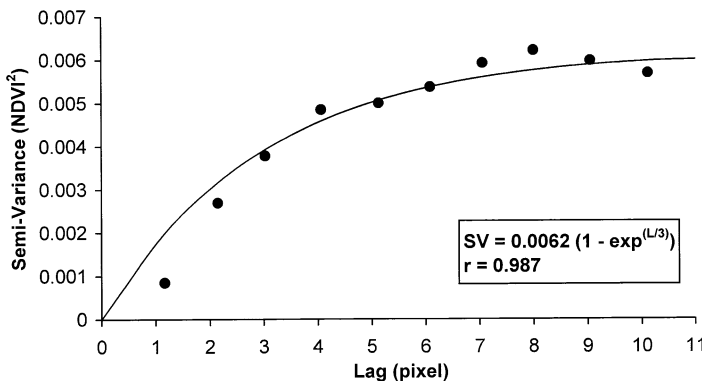


Figure 4. Experimental (points) and fitted (line) semivariograms obtained using the most spatially variable NDVI values of homogeneous areas.

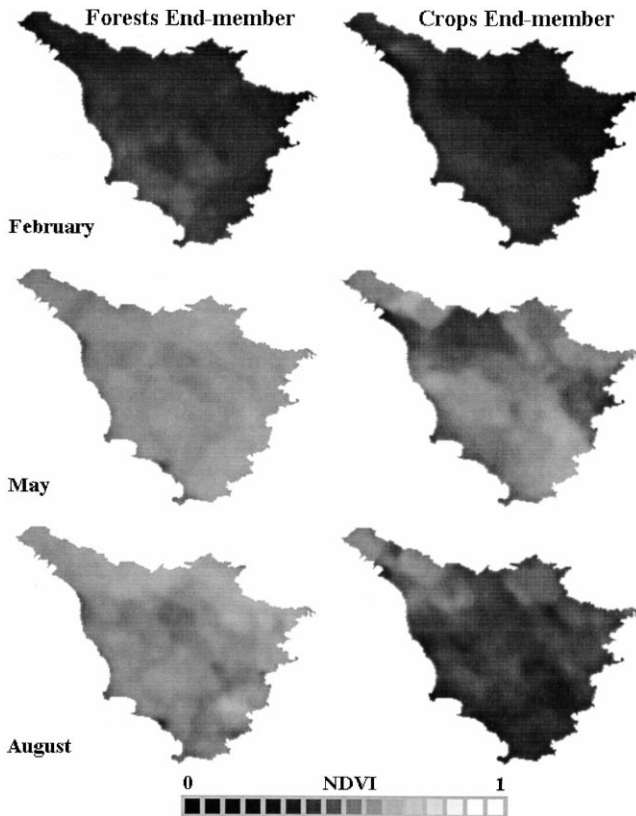


Figure 5. NDVI endmember images of two cover classes (forests and cereal crops) for three months (February, May, and August) found by the locally calibrated regression procedure.

analysis of the synthetic images indicated a higher spatial information content produced by the locally calibrated procedure. This was obviously expected, since the new procedure accounted for at least a part of the spatial variability contained in pure class NDVI data.

As previously explained, the accuracy of the reconstructed NDVI images was statistically evaluated by comparing them to the original monthly NDVI images. The r and RMSE values found for the two image series obtained by the conventional and locally calibrated multivariate regressions are reported in the histograms of Figs. 7A and 7B. It can be clearly noted that the new method produced correlation coefficients far higher than the conventional one, especially for winter months, where improvements in r higher than 0.5 were found. These improvements remained in terms of RMSE, but the seasonal differences were much less apparent, since all RMSEs decreased of 0.2 to 0.3 NDVI by using the new method.

These error patterns can be explained by considering that the NDVI ranges of the original images were much higher in the arid period than in the other seasons, due to the strong contrast between areas with low NDVI in the plains (where vegetation is limited by water availability) and with high NDVI on the mountains (Maselli et al., 1998b). This was partly taken into account also by the

conventional procedure, since, as can be seen in Fig. 3, forests had on average markedly higher NDVI values than the other vegetation classes in summer. These large summer ranges led to high r values by both methodologies and reduced the possible improvements obtainable by the new procedure in terms of this statistic. On the contrary, in winter, when all five conventionally found NDVI endmembers were similar, most NDVI variability was within cover classes, which was well accounted for only by the new method. The greater NDVI variability in summer is also reflected in the higher RMSE values obtained for this period by both procedures (Fig. 7B). In any case, the locally calibrated method always produced acceptable r (higher than 0.80) and RMSE (lower than 0.05 NDVI) values.

DISCUSSION AND CONCLUSIONS

The concept of spectral classes that are internally homogeneous and distinct from the others is one of the fundamentals of conventional image processing techniques (Richards, 1993). Recent investigations, however, have demonstrated that this concept is questionable in most real cases, since cover types are generally variable in structure and composition depending on a number of factors, while their boundaries are often graduating into those of the adjacent surfaces (Foody, 1992; Maselli et al., 1996). These considerations have led to the formulation of new approaches, such as fuzzy classification techniques, which take into account both intraclass spectral heterogeneity and interclass mixtures in relation to the spatial resolution of the data considered (Wang, 1990a; Wang, 1990b; Foody, 1992; Maselli et al., 1996).

Less work has been done regarding linear spectral mixing and unmixing theory and application. Linear unmixing methods have been shown to provide operational advantages over statistical classification procedures, since, on the basis of simple basic assumptions, they can efficiently produce information on a subpixel level (Settle and Drake, 1993). Moreover, these methods give a useful framework for the integration of data with different spectral, spatial, and temporal resolutions (Maselli et al., 1998a). Both linear mixing theory and unmixing procedures are based on the identification of the spectral signatures of pure materials or classes (spectral endmembers). For simplicity, spectral endmembers are generally considered unique and constant over the study images, neglecting the above-mentioned problems due to intraclass spectral variations (Settle and Drake, 1993). Only recently some research efforts have been directed to the consideration of variable spectral endmembers (Lacaze et al., 1996; Maselli, 1998), but without dealing with the problems related to their continuous spatial variability, which, as previously seen, may arise from several factors.

To address this important issue, an approach has been currently proposed that identifies spatially variable spectral endmembers. The approach is based on a modification

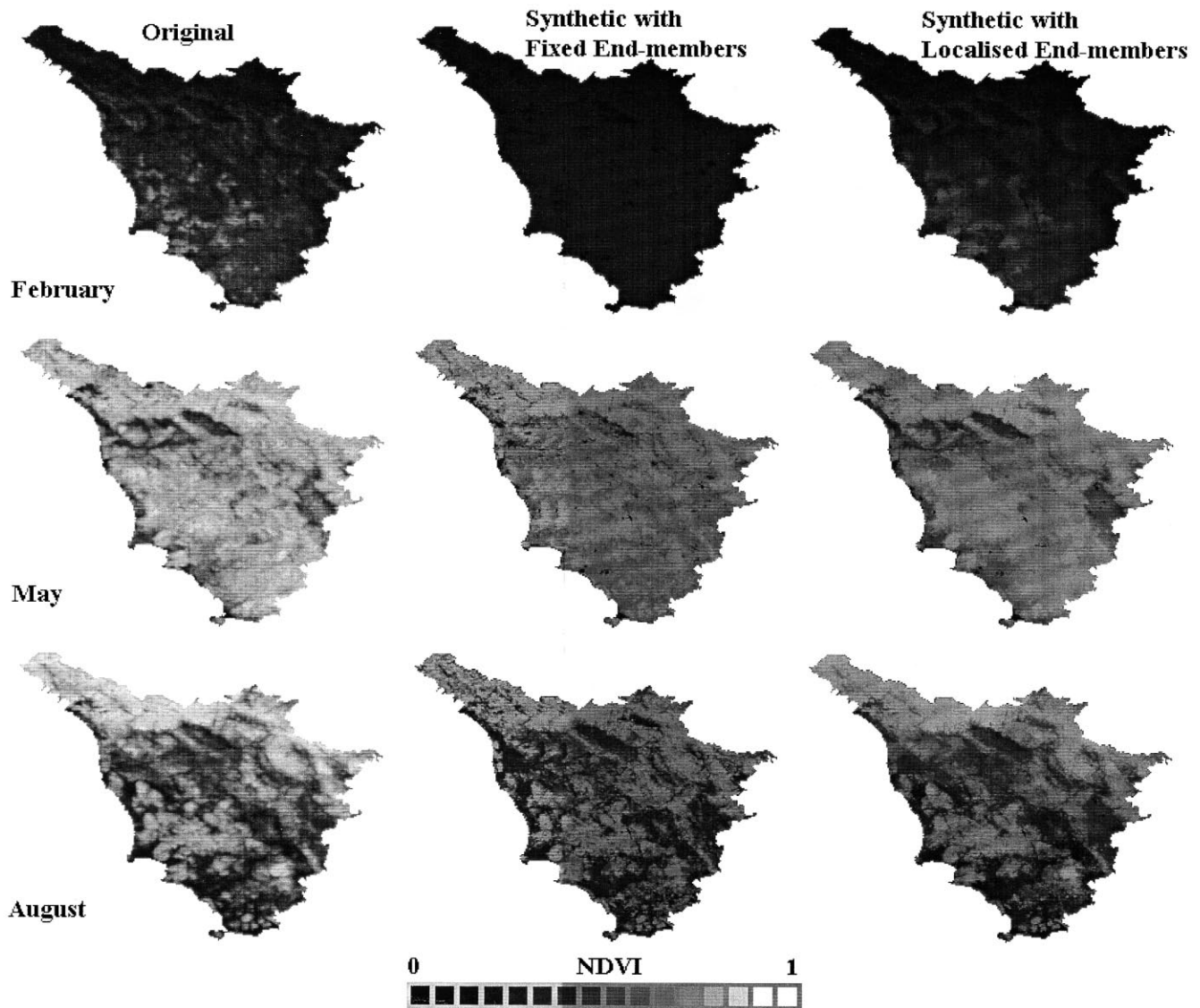


Figure 6. Original and synthetic NDVI images obtained by the two methods for the three exemplary months (February, May, and August).

of common multivariate regression procedures that are applied to identify spectral endmembers using abundance estimates (Kerdiles and Grondona, 1995; Maselli et al., 1998a). In practice, linear regression procedures are locally calibrated by computing on a per-pixel basis spatially variable regression statistics (mean vectors and variance/covariance matrices of both independent and dependent variables). The spectral endmembers found in this way express the pure signatures of each cover class for each study point. As was demonstrated in a case study, the method is efficient for providing local estimates of multitemporal endmembers that may vary in space due to the above-mentioned environmental factors. Similar results can be expected when applying the procedure to identify multispectral endmembers of materials or classes that are spatially heterogeneous.

From a practical viewpoint, the method could be used for numerous applications. For example, the locally calibrated endmembers could serve for a more efficient integration of data with different spatial and temporal features. In the case study currently examined, an NDVI data set with the spatial resolution of the CORINE land cover map (100 m) and monthly temporal frequency could be produced by applying a formula similar to Eq. (4) to the pure class NDVI estimates and the high resolution digital map (Maselli et al., 1998a). The advantage offered by the current method is that different NDVI values can be attributed to each cover class for different AVHRR pixels.

Such an integrated data set could directly serve for monitoring purposes (Sellers et al., 1995; Bolle, 1996), but could find its maximum utility as input for environmental modeling approaches. Multitemporal NDVI profiles of ag-

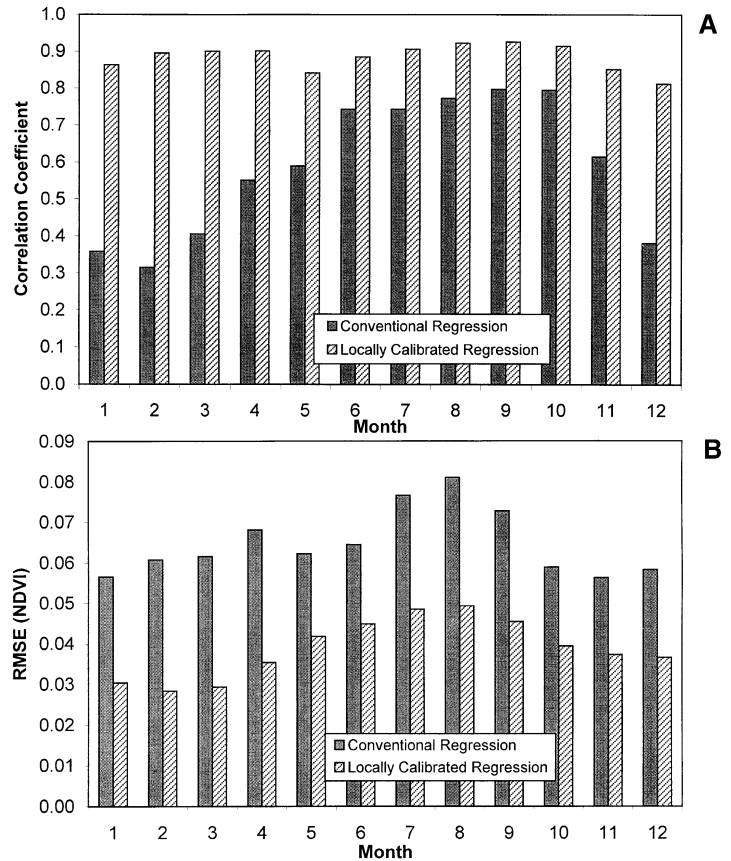


Figure 7. (A and B) Accuracy statistics (r and RMSE) found by comparing the original and synthetic NDVI images obtained by the two methods.

ricultural cover classes are in fact operationally utilized within agro-meteorological models for yield forecasting in North America (Doraiswamy et al., 1999) and Europe (Genovese et al., 1999). Most ecosystem simulation models, such as the well-known Forest BGC (Running and Coughlan, 1988; Kimball et al., 1997) also require as fundamental input variables Leaf Area Index estimates, which can be derived from NDVI data (Lacaze et al., 1996). In all these cases more accurate, locally defined NDVI estimates of pure classes could be of utmost importance. Research therefore is directed toward these applications, which should favor the operational utilization of the information coming from current and future satellite systems.

The research was partly funded by the Italian Space Agency (ASI) and by the EU project RESMEDES (Remote Sensing of Mediterranean Desertification and Environmental Stability). In particular, the author wishes to thank Nuova Telespazio S.p.A., Rome, for providing, within the framework of RESMEDES, the NOAA-AVHRR NDVI images used in the research. Thanks are also due to two anonymous RSE referees for their helpful comments on the first draft of the paper.

REFERENCES

- Anderson, T. W. (1984), *An Introduction to Multivariate Statistical Analysis*, 2d ed. John Wiley and Sons, New York.
- Annoni, A., and Perdigo, V. (1997), *Technical and Methodological Guide for Updating CORINE Land Cover Data Base*, European Commission, EUR 17288EN, Space Application Institute of Joint Research Centre, Ispra, Italy.
- Bateson, A., and Curtiss, B. (1996), A method for manual end-member selection and spectral unmixing. *Remote Sens. Environ.* 55:229–243.
- Bolle, H. J. (1996), The role of remote sensing in understanding and controlling land degradation and desertification processes: The EFEDA research strategy. In *The Use of Remote Sensing for Land Degradation and Desertification Monitoring in the Mediterranean Basin. State of the Art and Future Research* (J. Hill and D. Peter, Eds.), Directorate-General Science, Research and Development, European Commission, pp. 45–77.
- Davis, J. C. (1973), *Statistics and Data Analysis in Geology*. Wiley, New York.
- Doraiswamy, P. C., Zara, P. M., and Stern, J. (1999), Application of a crop simulation model for assessment of regional crop production. In *Proceedings of the International Symposium "Modelling Cropping Systems,"* Lleida (Spain), 21–23 June 1999, pp. 167–168.
- Foody, G. M. (1992), A fuzzy sets approach to the representation of vegetation continua from remotely sensed data: an example from Lowland Heath. *Photogramm. Eng. Remote Sens.* 58:221–225.
- Gaston, G. G., Jackson, P. L., Vinson, T. S., Kolchugina, T. P., Botch, M., and Kobak, K. (1994), Identification of carbon quantifiable regions in the former Soviet Union using unsuper-

- vised classification of AVHRR global vegetation index images. *Int. J. Remote Sens.* 15:3199–3221.
- Genovese, G., Vignolles, C., Nègre, T., and Passera, G. (1999), The use of CORINE land cover to improve vegetation monitoring through NOAA-AVHRR/NDVI profiles. In *Proceedings of the International Symposium "Modelling Cropping Systems,"* Lleida (Spain), 21–23 June 199, pp. 83–84.
- Gilabert, M. A., Conese, C., and Maselli, F. (1994), An atmospheric correction method for the automatic retrieval of surface reflectances from TM images. *Int. J. Remote Sens.* 15: 2065–2086.
- Holben, B. N. (1986), Characteristics of maximum-value composite images from temporal AVHRR data. *Int. J. Remote Sens.* 7:1417–1434.
- Kerdiles, H., and Grondona, M. O. (1995), NOAA-AVHRR NDVI decomposition and subpixel classification using linear mixing in the Argentinean Pampa. *Int. J. Remote Sens.* 16:1303–1325.
- Kimball, J. S., Thornton, P. E., White, M. A., and Running, S. W., (1997), Simulating forest productivity and surface-atmosphere exchange in the BOREAS study region. *Tree Physiol.* 17: 589–599.
- Lacaze, B., Caselles, V., Coll, C., Hill, H., Hoff, C., de Jong, S., Mehl, W., Negendank, J. F. W., Riesebos, H., Rubio, E., Sommer, S., Teixeira Filho, J., and Valor, E. (1996), *DeMon*—Integrated approaches to desertification mapping and monitoring in the Mediterranean basin, *Final Report of DeMon-1 Project*, Joint Research Centre of European Commission, Ispra (VA), Italy.
- Los, S. O. (1998), *Linkages between Global Vegetation and Climate. An Analysis Based on NOAA Advanced Very High Resolution Radiometer Data*, PhD. Dissertation, Vrije Universiteit, Goddard Space Flight Centre, Greenbelt, MD.
- Maselli, F., Rodolfi, A., and Conese, C. (1996), Fuzzy classification of spatially degraded TM data for the estimation of subpixel components. *Int. J. Remote Sens.* 17:537–551.
- Maselli, F., Gilabert, M. A., and Conese, C. (1998a), Integration of high and low resolution NDVI data for monitoring vegetation in Mediterranean environments. *Remote Sens. Environ.* 63:208–218.
- Maselli, F., Petkov, L., and Maracchi, G., (1998b), Extension of climate parameters over the land surface by the use of NOAA-AVHRR and ancillary data. *Photogramm. Eng. Remote Sens.* 64:199–206.
- Maselli, F. (1998), Multiclass spectral decomposition of remotely sensed scenes by selective pixel unmixing. *IEEE Transact. Geosci. Remote Sens.* 36:1809–1820.
- Oleson, K. W., Sarlin, S., Garrison, J., Smith, S., Privette, J. L., and Emery, W. J. (1995), Unmixing multiple land-cover type reflectances from coarse spatial resolution satellite data. *Remote Sens. Environ.* 54:98–112.
- Pannatier, Y. (1994), MS-WINDOWS Programs for Exploratory Variography and Variogram Modeling in 2D. In *Statistics of Spatial Processes: Theory and Applications* (V. Capasso, G. Girone, and D. Posa, Eds.), Bari, Italy, pp. 165–170.
- Puyou-Lascassies, P., Flouzat, G., Gay, M., and Vignolles, C. (1994), Validation of the use of multiple linear regression as a tool for unmixing coarse spatial resolution images. *Remote Sens. Environ.* 49:155–166.
- Rao, C. R. N., and Chen, J. (1994), Post-launch calibration of the visible and near infrared channels of the Advanced Very High Resolution Radiometer on NOAA-7, -9, and -11 spacecraft, *NOAA Technical Report NESDIS 78*, U.S. Department of Commerce, Washington, D.C., August 1994.
- Rapetti, F., and Vittorini, S. (1995), *Carta Climatica Della Toscana Centro-Meridionale e Insulare*. Pacini Editore, Pisa, Italy.
- Richards, J. A. (1993), *Remote Sensing Digital Image Analysis: An Introduction*, 2d ed. Springer-Verlag, Heilderberg.
- Rossini, P., Bottai, L., Frezzotti, M., Pandiscia, G., and Taddei, R. (1994), Nuova Telespazio contribution to Annual Progress Report of EFEDA-Phase II, *E.C. Project EFEDA, Group V, Remote Sensing and Radiometric Properties of the Surface: Assessment of Desertification from Space*, Coordinator H. J. Bolle, Berlin, November 1994.
- Running, S. W., and Coughlan, J. C. (1988), A general model of forest ecosystem processes for regional applications. *Ecological Modelling* 42:125–154.
- Sellers, P. J., Meeson, B. W., Hall, F. G., Asrar, G., Murphy, R. E., Schiffer, R. A., Bretherton, F. P., Dickinson, R. E., Ellingson, R. G., Field, C. B., Huemmrich, K. F., Justice, C. O., Melack, J. M., Roulet, N. T., Schimel, D. S., and Try, P. D. (1995), Remote sensing of the land surface for studies of global change: Models—algorithms—Experiments. *Remote Sens. Environ.* 51:3–26.
- Settle, J. J., and Drake, N. A. (1993), Linear mixing and the estimation of ground cover proportion. *Int. J. Remote Sens.* 14:1159–1177.
- Shimabukuru, Y. E., and Smith, J. A. (1991), The least squares mixing models to generate fraction images derived from remote sensing multispectral data. *IEEE Transact. Geosci. Remote Sens.* 29:16–20.
- Smith, M. O., Ustin, S. L., Adams, J. B., and Gillespie, A. R. (1990), Vegetation in deserts: A regional measure of abundance from multispectral images. *Remote Sens. Environ.* 31:1–26.
- Tompkins, T., Mustard, J. F., Pieters, C. M., and Forsyth, D. W. (1997), Optimization of endmembers for spectral mixture analysis. *Remote Sens. Environ.* 59:472–489.
- Townshend, J. R. G. (1994), Global data sets for land applications from the Advanced Very High Resolution Radiometer: an introduction. *Int. J. Remote Sens.* 15:3319–3332.
- Wang, F. (1990a), Fuzzy supervised classification of remote sensing images. *IEEE Transact. Geosci. Remote Sens.* 28:194–201.
- Wang, F. (1990b), Improving remote sensing image analysis through fuzzy information representation. *Photogramm. Eng. Remote Sens.* 56:1163–1169.
- Woodcock, C. E., and Strahler, A. H. (1987), The factor of scale in remote sensing. *Remote Sens. Environ.* 21:311–332.
- Van der Meer, F. (1999), Iterative spectral unmixing. *Int. J. Remote Sens.* 20:3431–3436.
- Zadeh, L. A. (1965), Fuzzy sets. *Inf. and Cont.* 8:338–353.